Ultra Wideband Wireless Body Area Network for Medical Applications

I. Balasingham[1,2,3], **R. Chávez-Santiago**[1,2], **J. Bergsland**[1], **T.A. Ramstad**[2] **and E. Fosse**[1,3]
[1] The Interventional Centre, Oslo University Hospital
Sognsvannsveien 20, Oslo N-0027, Norway
[2] Department of Electronics and Telecommunications
Norwegian University of Science and Technology (NTNU), Trondheim N-7491, Norway
[3]Institute of Clinical Medicine
University of Oslo, Oslo N-0316, Norway

Ilangko.Balasingham@medisin.uio.no

ABSTRACT

The utilization of wireless technology in traditional medical services provides patients with enhanced mobility. This has a positive effect in the recovery speed of a person after major surgical procedures or prolonged illness. Ultra wideband (UWB) radio signals have inherent characteristics that make them highly suitable for less invasive medical applications. This paper surveys our recent research on UWB technology for medical sensing, imaging, and localization. The interconnection of multiple wireless sensors that constitute a medical body area network (WBAN) is also described. Research perspectives in the aforementioned topics are suggested too.

1.0 INTRODUCTION

In the last years there has been an increasing interest in using ultra wideband (UWB) technology for wireless communication interfaces [1]. The IEEE 802.15.4a standard has adopted UWB as one of the interfaces for robust low data rate transmission in wireless personal networks (WPANs) with precision ranging capabilities [2]. UWB signals have an inherent noise-like behaviour due to their extremely low maximum effective isotropically radiated power (EIRP) spectral density of –41.3 dBm/MHz. This makes them difficult-to-detect and robust against jamming, potentially rescinding the need for complex encryption algorithms in tiny transceivers. Owing to these characteristics, UWB has emerged as a solution for the radio interface in low data rate medical wireless sensor networks (WSNs) [3]. Additionally, UWB signals do not cause significant interference to other systems operating in the vicinity and do not represent a threat to patients' safety [4]. Impulse radio (IR) transceivers have simple structure and very low power consumption, which facilitates their miniaturization [5]–[7].

A promising application of UWB as wireless interface is in the field of capsule endoscopy. A capsule endoscope is a camera with the size and shape of a pill that is swallowed in order to visualize the gastrointestinal tract. They originally were devised to transmit still images of the digestive tract for subsequent diagnosis and detection of gastrointestinal diseases. Nevertheless, real-time video imaging of the digestive tract is feasible using an UWB radio interface [8]. Although capsule endoscopy is an invasive technique, it provides the patient with more comfort than traditional endoscopy and colonoscopy. Capsule endoscopy has demonstrated the ability to detect diseases in the small intestine in cases in which other techniques cannot [9]–[11].

Besides being used as wireless communication interface, UWB technology has many other possible applications in healthcare systems [12]. For instance, the IR-UWB radar has the potential capability to detect, noninvasively, tiny movements inside the human body [13]. It is entirely possible to monitor cardiovascular physiological parameters using movement detection of the aorta [14] or other parts

Report Documentation Page

Form Approved
OMB No. 0704-0188

1. REPORT DATE	2. REPORT TYPE	3. DATES COVERED
APR 2010	**N/A**	**-**

4. TITLE AND SUBTITLE	5a. CONTRACT NUMBER
Ultra Wideband Wireless Body Area Network for Medical Applications	5b. GRANT NUMBER
	5c. PROGRAM ELEMENT NUMBER
6. AUTHOR(S)	5d. PROJECT NUMBER
	5e. TASK NUMBER
	5f. WORK UNIT NUMBER
7. PERFORMING ORGANIZATION NAME(S) AND ADDRESS(ES) **The Interventional Centre, Oslo University Hospital Sognsvannsveien 20, Oslo N-0027, Norway**	8. PERFORMING ORGANIZATION REPORT NUMBER
9. SPONSORING/MONITORING AGENCY NAME(S) AND ADDRESS(ES)	10. SPONSOR/MONITOR'S ACRONYM(S)
	11. SPONSOR/MONITOR'S REPORT NUMBER(S)

12. DISTRIBUTION/AVAILABILITY STATEMENT
Approved for public release, distribution unlimited

13. SUPPLEMENTARY NOTES
See also ADA564622. Use of Advanced Technologies and New Procedures in Medical Field Operations (Utilisation de technologies avancees et de procedures nouvelles dans les operations sanitaires).

14. ABSTRACT
The utilization of wireless technology in traditional medical services provides patients with enhanced mobility. This has a positive effect in the recovery speed of a person after major surgical procedures or prolonged illness. Ultra wideband (UWB) radio signals have inherent characteristics that make them highly suitable for less invasive medical applications. This paper surveys our recent research on UWB technology for medical sensing, imaging, and localization. The interconnection of multiple wireless sensors that constitute a medical body area network (WBAN) is also described. Research perspectives in the aforementioned topics are suggested too.

15. SUBJECT TERMS

16. SECURITY CLASSIFICATION OF:			17. LIMITATION OF ABSTRACT	18. NUMBER OF PAGES	19a. NAME OF RESPONSIBLE PERSON
a. REPORT	b. ABSTRACT	c. THIS PAGE			
unclassified	**unclassified**	**unclassified**	**SAR**	**24**	

of the arterial system. Such parameters include heart rate (HR), respiration related motion, blood pressure (BP), etc. Due to the architecture of the UWB radar, it is feasible to use the same transceiver for both radar sensing and IR-UWB communications [7].

Imaging of surface and more deeply located structures such as breast tissue for cancer diagnosis is another promising application of UWB technology [15]–[21]. This has the potential of taking over the role of X-Ray mammography. The great advantage will be the absence of ionizing radiation, which poses a certain cancer risk when used repeatedly. In the same vain, UWB imaging has the potential to be used in diagnosing skin cancer as it can provide information of morphological and physiological changes in the dermal tissues.

The rest of the paper is organized as follows: Section 2 provides a summary of our current research on UWB invasive and noninvasive medical sensing; an overview of UWB imaging for early breast cancer detection is also included. Section 3 consists of a short overview of sensor localization techniques in a wireless body area network (WBAN). Section 4 describes the network architecture to interconnect noninvasive and invasive sensors using UWB radio interfaces. Finally, our conclusions are summarized in Section 5.

2.0 MEDICAL SENSING AND IMAGING USING UWB TECHNOLOGY

This Section presents a summary of our research on medical sensing, both invasive and noninvasive. The temporarily-invasive sensing technique that we are currently pursuing is the use of UWB for the communication link of a capsule endoscope system. Immediately after the capsule endoscope description, a feasibility study for noninvasive BP measurements using UWB radar is presented. A survey of UWB imaging for early breast cancer detection is included; research perspectives in each field are suggested.

2.1 Capsule Endoscopy

Traditional medical practice for the diagnosis of patients with disorders such as unexplained anal bleeding, Crohn's disease, Celiac disease, and intestinal tumours relies on the insertion of flexible tubes containing cameras to examine parts of the digestive tract. This technique, however, can examine the upper portion of the digestive tract only, while colonoscopes help to visualize the lower part (colon). There is a large portion (approx. 6 meters) of the small intestine that cannot be inspected with these traditional techniques. Capsule endoscopes help to fill this gap with less discomfort for the patient.

State-of-the-art capsule endoscopes are swallowed with water, after which the patient put a recorder belt on his/her waist. Some hours later (typically eight), medical staff look for abnormalities by reviewing a video created from the still images transmitted wirelessly from the capsule endoscope to the recorder belt. Adding the capability to transmit and analyze video in real time can provide further flexibility and advantages to the current technology. This additional capability, however, might increase the complexity of the circuitry and hence the power consumption of the capsule endoscope. The power consumption of a capsule endoscope must be as low as possible, on the order of 1 mW, with a mandatory small physical size on the order of 300 cubic millimetres. Transmitting real-time video requires a high data rate communication link, on the order of 73.8 Mbps for uncompressed VGA data. All these requirements are hard to achieve using narrowband (NB) systems that operate in the medical implant communication systems (MICS) frequency band of 402–405 MHz. In contrast, UWB technology has the potential to fulfil them all.

2.1.1 Communication System Architecture

UWB communications can be implemented using multi-band orthogonal frequency division multiplexing (MB-OFDM), direct-sequence spread spectrum (DSSS) and *impulse radio*. The MB-OFDM and DS-UWB

transceivers need frequency carriers for up-and down-conversion of the baseband signal. Therefore, a frequency synthesizer is necessary, which increases the complexity and power consumption of the system. IR-UWB, on the other hand, directly modulates the information bits with extremely short-duration pulses. Since the pulse occupies a large bandwidth (no less than 500 MHz), it can be directly emitted without using carriers or any intermediate frequency (IF) processing, greatly reducing the system complexity and the overall power consumption and size [22]. A capsule endoscope communication system includes an in-body transmitter and an on-body receiver with its corresponding blocks for synchronization and base-band processing.

2.1.1.1 In-Body Transmitter

Due to limitations at the in-body transmitter including power consumption, size, system cost and complexity, its communication architecture must be as simple as possible (Figure 1).

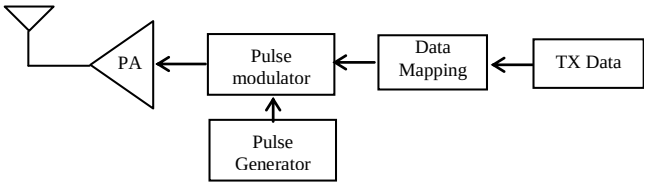

Figure 1: UWB Transmitter Block Diagram for a Capsule Endoscope System.

A pulse generator provides the UWB pulse that is subsequently modulated, amplified and transmitted. The shape of the transmitted pulse determines the signal bandwidth. We use the fifth derivative of a Gaussian pulse to cover a bandwidth of approximately 1–5 GHz. The power spectral density (PSD) of the transmitted pulse is shown in Figure 2.

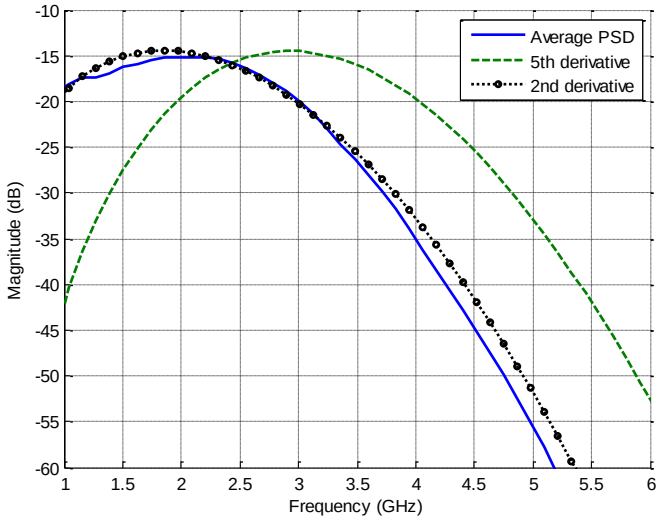

Figure 2: PSD of the Transmitted Gaussian Pulse (Fifth Derivative), the Averaged PSD of In-Body Channel Realizations, and the Fitted Second Derivative Gaussian Pulse Signal.

The generated data from the electro-optical circuitry of the capsule endoscope can be processed for data compression and coding or can be directly modulated without further processing thus simplifying the transmitter architecture. The modulation is performed by changing the characteristics of the generated

pulse. We consider the bi-phase pulse amplitude modulation (BPAM) scheme, in which the data bits are expressed by the polarity of the transmitted pulses. The resulting signal is then amplified and transmitted. The transmitter antenna must cover the entire frequency range with little pulse distortion. The design of a compact UWB antenna for the in-body transmitter is a challenging task that has opened a new field of research activities [23].

2.1.1.2 On-Body Receiver

For the on-body receiver we propose a novel architecture, which uses a single branch correlator (including a multiplier and an integrator) for recovering the transmitted signal. The block diagram of the receiver is depicted in Figure 3.

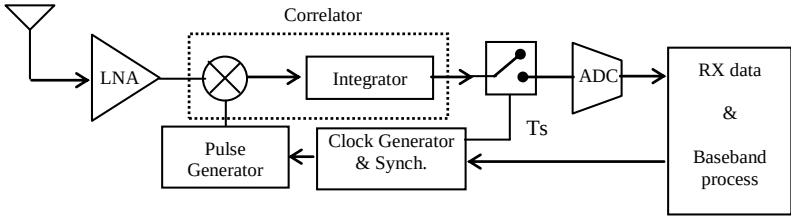

Figure 3: UWB Receiver Block Diagram for a Capsule Endoscope System.

The UWB antenna at the receiver can be placed on the skin or at some distance away. By placing the receiving antenna on the body surface, the nonradiative near-field components can be collected by the antenna thus improving the link quality significantly. We have found an improvement of 6 dB due to near-field coupling in UWB in-body links [24]. The practical implementation of the receiver antenna requires a special antenna structure since it must cover a relatively wide body area (abdominal torso). Commonly, a spatial-diversity antenna array around the torso is embedded in a recorder belt, which is worn by the patient while the capsule endoscope operates. A less invasive receiver can be attained by placing the antenna at some distance away the skin; in such case, extra free-space path loss is added and the near-field coupling gain is lost. However, a high-gain antenna can be used to compensate for a portion of these losses. For example, a double ridged horn antenna structure with coverage of the whole abdomen area can be considered.

The low noise amplifier (LNA) increases the power of the received pulses to a suitable level for signal processing and to overcome noise in subsequent electronic stages. The data are subsequently recovered by the correlator. The correlation operation can be implemented in either analog or digital circuits. Using an all-digital receiver requires highly sophisticated receiver processors with an analog-to-digital converter (ADC) with sampling rate of 2 or 4 times that of the pulse bandwidth and resolution of 4-6 bits. A hybrid analog and digital receiver can reduce the system complexity and cost by decreasing the sampling rate and resolution of the ADC [25]. Although an analog solution is prone to suffer from desensitization and other third-order distortions caused by nonlinearities in the electronic circuits, the use of state-of-the-art high-linearity UWB electronics in 0.18 μm CMOS technology [26], [27] can reduce this problem almost completely. Hence, for simplicity we ignore the effects of circuitry nonlinearities. The correlator output is then sampled and the ADC converts the analog demodulated signal into digital form. The digital baseband circuitry provides control for the clock generation, synchronization, and data processing.

One might think that the receiver can take advantage of multipath signals by creating a bank of correlators (Rake receiver structure). This idea has been applied to IR-UWB links in dispersive channels with large number of correlators and more complicate system. However, the imperfect correlations resulting from distorted received pulses reduce the system performance. An optimal way to correct this problem is using a template-match detection technique that performs a matched filter operation with a series of template

waveforms. However, the system complexity increases significantly and channel estimation is required. Hence, we propose using a *single branch correlator* with an optimized pre-defined template that guarantees maximum energy recovery. The associated delay of the template is adjusted so that maximum correlator output at one branch is generated. The short root-mean-square (RMS) delay spread of in-body channels (on the order of 1 ns) [28] enables this simple architecture.

The design of the pre-defined template depends on the propagation channel characteristics. By multiple electromagnetic (EM) simulations of UWB signals propagating through the abdomen, the normalized average PSD of the "digestive" radio channel was obtained (see Figure 2). The second derivative of a Gaussian pulse can approximate fairly well the radio channel PSD and therefore is chosen as the pre-defined template. It is important to mention, however, that this template pulse choice is optimal for the ideal case that we considered so far in which the antenna effects were disregarded. Taking into account the antenna effects would have a considerable impact on the optimal template. In such case, the EM simulations must include the particular antenna specifications in order to select the most appropriate template for any other specific design.

2.1.2 Performance Evaluation

The maximum correlator output is attained under the synchronization scheme described in [29]. Considering the received distorted signal as $r(t - kT_s)$ and the noise signal as $n(t)$, the correlator output signal, C_k, can be expressed as

$$C_k = R_k + N_k,$$

$$R_k = a_k \int_{-\infty}^{+\infty} r(t - kT_s)\, p(t - kT_s - \tau)\, dt,$$

$$N_k = \int_{-\infty}^{+\infty} n(t)\, p(t - kT_s - \tau)\, dt,$$

where a_k is the *k*-th data bit {±1}, $p(t)$ is the template signal, τ is the delay and T_s is the bit duty cycle. The correlator output is sampled at the synchronized (maximum) position to recover the polarity of the received data bits. Due to the correlation process and the signal sampling at the maximum correlator output, the signal-to-noise ratio (SNR) is significantly improved and can be expressed as

$$\text{SNR} = \frac{|R_k|^2}{E\left(|N_k|^2\right)} = \eta \frac{P_{rx}}{N_0},$$

where N_k is a zero mean random variable with Gaussian distribution, $E(\bullet)$ is the expectation operation, P_{rx} is the average received power, N_0 is the noise power density and η is the maximum output of the correlator at $\tau = \tau_{\max}$, defined as

$$\eta = \left(\int_{-\infty}^{+\infty} \frac{r(t)}{\sqrt{\int_{-\infty}^{+\infty} |r(t)|^2 dt}} \frac{p(t - \tau_{\max})}{\sqrt{\int_{-\infty}^{+\infty} |p(t)|^2 dt}} \right)^2.$$

The average bit-error-rate (BER) performance (averaged over 90 arbitrary link realizations) for different templates in an additive white Gaussian noise environment is compared in Figure 4. The worst performance is observed using the fifth derivative of the Gaussian pulse as template. The reduced BER performance reveals significant distortion of the transmitted pulse while propagating through the body tissues. The best BER performance is obtained for the second derivative, which collects more signal energy from the distorted pulses. For a typical BER of 10^{-3}, a mismatch loss of 5 dB is observed with respect to the ideal case. Using the first and the third derivatives provide almost similar BER performance.

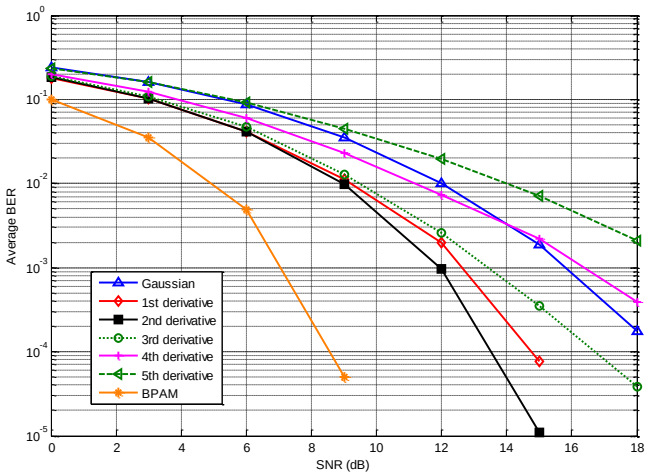

Figure 4: Averaged BER Performance Using Different Templates.

2.1.3 Research Perspectives

Additional simulations [29] have demonstrated the feasibility of transmitting information at very high data rates (up to 100 Mbps) with the communication architecture described above. These results encourage research toward the improvement of our current design. A major further step in capsule endoscopy will be the development of a full-duplex communication link. This means integrating not only a transmitter but also a receiver (transceiver architecture) in the capsule endoscope. This will allow transmitting external commands (movement, optical focus on specific areas, etc.) to the capsule endoscope thereby adding more control and flexibility to the device. The same transceiver can be used to remotely control microrobotic multifunctional endoscopic devices, capable of performing several diagnostic and therapeutic operations such as biopsy, electrocautery, laser microsurgery, etc. with a retractable arm [30]. The Interventional Centre (IVS) in Norway, http://www.ivs.no/, is currently pursuing the establishment of international cooperation for the design and implementation of such UWB transceiver, which represents a big challenge in nanoelectronics and antenna technology.

2.2 Blood Pressure Measurement

Noninvasive measurements of BP exist such as sphygmomanometer, photoplethysmograph [31], tonography [32], and pulse transit time [33]; however, they all rely on peripheral measurement points. This may constitute a problem in certain situations such as when flow redistribution to central parts of the body (heavy injury, temperature) degrades these measurements; another situation where central measurements may prove advantageous is in the presence of strong movement of the peripheral locations, which affects pressure measurements [34].

An interesting overview of the use of radar for medical applications can be found in [35], which traces research in the field back to the late 1970s. It seems that renewed interest has been spurred following the

micropower impulse radar in the mid-1990s [36], which combined UWB pulses with very low power, small size, and low system cost. The research into medical sensor applications include apexcardiography, heart rate, respiration rate, heart-rate variability, blood pressure pulse transit time (peripheral locations) and associated applications such as through-rubble or -walls vital signs detection [35]–[37].

The use of radar techniques to measure BP may draw upon ideas from these fields, as well as from ground penetrating radar (GPR), yet is sufficiently different to merit a specific approach; in particular, the complexity of geometry and stronger attenuation compared with early detection of breast cancer and as for heart and respiration rate measurements, which are essentially based on shallow reflections.

Estimating BP using radar techniques is necessarily indirect; pressure only affects propagation through the geometry unless it affects material EM properties, which is not expected. In the case of the aortic BP, two effects may relate aorta diameter (geometry) to its pressure:

- Using the linear relationship between percentage changes in instantaneous BP and diameter, shown for carotid artery pressure in [38];
- Estimating the elasticity of the aorta (local compliance or incremental elastic modulus) and relating this to BP [33], [34], [39] without being explicit with respect to the functional relationship.

In both approaches, the radar-based method will aim at detecting the aorta walls and estimate the diameter as a function of time, $d(t)$.

2.2.1 Feasibility Study

From a medical point of view, central measurements are better than peripheral ones. Therefore, we pursue the measurement of BP through movement detection of the aorta. In order to understand the principles of using UWB radar to measure aorta diameter variations, a simple model was constructed for EM simulations [14]. Our model combines a voxel representation of the human body with the material dielectric properties proposed in [40]. It is based on a 2D simplified geometry: a cylinder of diameter *d* (representing the aorta) immersed in a lossy medium (Figure 5). The lossy medium approximates average living tissue dielectric properties, except for the skin and aorta, the properties of which are taken from [40]. Further details of the model and the EM simulations can be found in [14].

With diameter variations on the order of 2 mm, a set of simulations with aorta diameter ranging from 20 mm to 26 mm in steps of 0.4 mm were conducted in a simulation space with a resolution of 0.1 mm. The current source signal in the simulations was the seventh derivative of a Gaussian pulse with energy centred around 4.5 GHz. This relatively high-order derivative was mainly used for compensating, to a certain extent, the frequency-dependant attenuation in the simulations.

The analysis of the resulting transfer function and the time-domain echoes led to the conclusion that the backscattered signal from the aorta contains necessary information for distinguishing front and rear walls of the aorta thereby making the estimation of its diameter feasible. However, due to strong attenuation in living tissues, feasibility is essentially hinged on a viable power budget. In the simulations, an upper bound on received power in the 0.8–5 GHz range shows a 40 dB loss at the lower end increasing to about 120 dB at the upper end where material loss is dominant.

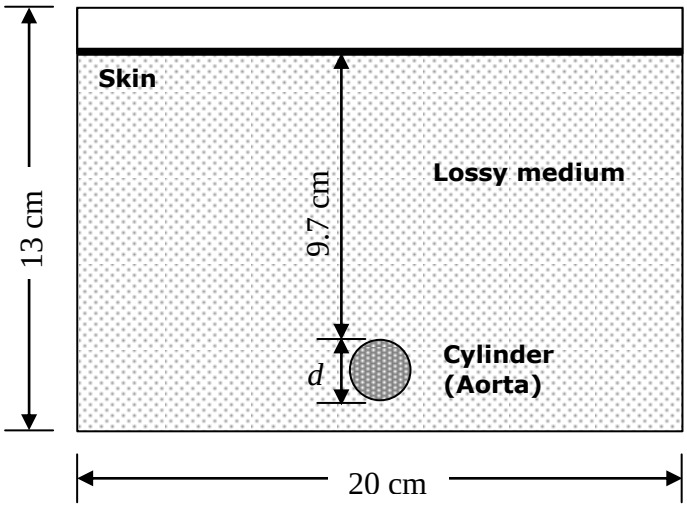

Figure 5: 2D Simulation Model for Aorta's Diameter Estimation.

2.2.2 Research Perspectives

There are several tradeoffs involved in achieving BP measurements with UWB radar: high-frequency content versus SNR at the receiver as tissues generally severely attenuate the signals; high-frequency versus resolution (and signal-to-clutter reduction) for the same reason. Hence, our current research effort is focused on identifying a criterion for the best selection of bandwidth and centre frequency. Another key issue that needs to be addressed is whether the use of an antenna array may improve measurement, and if so, how much and in which way should this best be implemented. Potentially, the use of an array introduces spatial selectivity and may improve the signal-to-clutter ratio.

Our ongoing research toward the demonstration of BP measurements using UWB radar is focused on the construction of a physical phantom model for estimation of the aorta diameter with sets of static measurements. This will allow for direct comparison between theoretic and practical results.

HR, respiration rate, and heart movements recording have already been proved feasible using IR-UWB radar [41], [42]. Several other possible medical applications of UWB radar include ambulatory cardiac output monitoring, blood vessel movement recording, blood pressure celerity measurement, and shock diagnosis in emergency patients. Similar technology can obviously be applied to pneumology and polysomnography for apnoea monitoring in infants, obstructive sleep apnoea monitoring, allergy and asthma crisis monitoring, etc. The application of UWB radar in obstetrics as a replacement for ultrasound has also been proposed [13], but this idea has been looked upon cautiously because of the great concern regarding radiofrequency (RF) safety for the newborn. Nevertheless, UWB radar can offer the medical staff and patients several advantages over ultrasound, such as noncontact operation, no need for cleaning after use, remote and continuous operation, lower cost, and easier operation. Intensive research will verify the subsequent clinical viability of UWB radar and acceptability of the technique.

2.3 Early Cancer Detection

Breast cancer continues being one of the main causes of women death; therefore, early detection of cancerous tumours increases the possibility of successful treatment and survival. Although a large number of detection methods are available, X-Ray mammography is currently the most widely used [43]. Nevertheless, despite its ability to provide high resolution images, this method suffers from high false-alarm rate and the incapability to distinguish between malignant and benignant tumours [44]. Additionally, the ionizing radiation used for imaging damages surrounding tissues and, overall, it is a painful and

uncomfortable experience for the patience. In recent years there has been an increasing interest in using high-resolution UWB radar for early breast cancer detection based on microwave imaging. This technology has the potential to overcome in a cost-effective way the limitations of X-Ray mammography.

UWB radar medical imaging involves transmitting an extremely short pulse through the breast tissues and then records the backscattered signal from different locations. The basis for detecting and locating a cancerous tumour is the different dielectric properties of healthy and malignant breast tissue. Healthy tissue is largely transparent to microwaves, whereas tumours, which contain more water and blood, scatter them back to the probing antenna array [18].

Preliminary results have been reported using near-field tomographic image reconstruction (TIR) [45], confocal microwave imaging [46], space-time beamforming [47], generalized likelihood ratio test based detection [48], and time-of-arrival (TOA) data fusion method [17]. Until recently, the tumour detection capabilities of various imaging techniques are evaluated through finite-difference time-domain (FDTD) methods [16]. Different phantom models for EM simulations have been proposed in the literature.

2.3.1 2D Breast Phantom Models

In [16] a 2D canonical breast model with average dielectric properties is proposed. The various tissues are considered nondispersive and the skin layer is omitted. As depicted in Figure 6, the model is a semicylinder centred at the origin with radius r_b. All the structures (clutter sources, glands, and ducts) are assumed to be infinitely long and uniformly distributed within the breast. The dielectric constant (permittivity) and conductivity of the average breast tissue are ε_b and σ_b, whereas for the clutter structures are $(1\pm\gamma)\varepsilon_b$ and $(1\pm\gamma)\sigma_b$, respectively, where γ denotes the mean percentage variation about the mean value; $+\gamma$ and $-\gamma$ are equally probable. Mamary glands and ducts can be added by uniformly positioning a group of cylinders with higher percentage variation $+\gamma'$. The tumour is modelled as a small cylinder interposed in the breast phantom with parameters ε_t and σ_t.

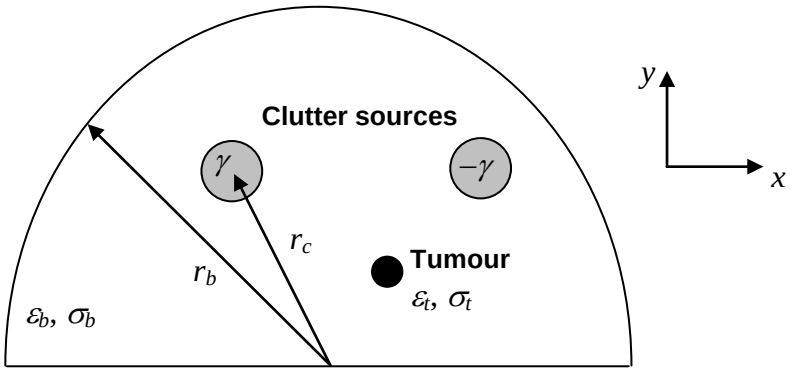

Figure 6: A Canonical 2D Breast Phantom Model.

Reported values for this model are $\varepsilon_b = 21.5$, $\sigma_b = 1.66$ S/m, $\varepsilon_t = 50.73$, $\sigma_t = 4.82$ S/m, and $\gamma = 30\,\%$. Typical values for the diameter of clutter sources and tumours are 4 mm and 2 mm, respectively, whereas $r_b = 50$ mm.

A model that considers specific tissues properties is presented in [20], but with a much simpler planar geometry (Figure 7) that is aimed to represent the naturally flattened breast when the patient is oriented in a supine position [46].

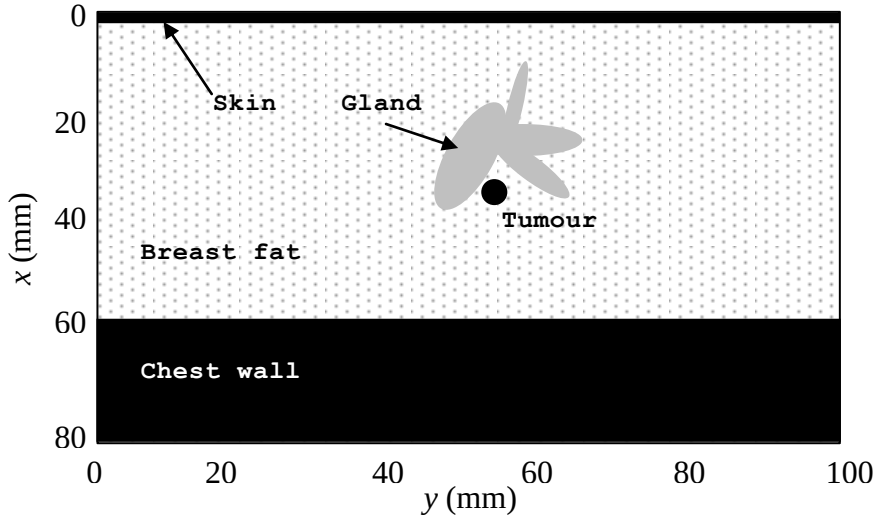

Figure 7: Geometry Configuration of the Planar Breast Structure.

The top surface of the structure is the 2 mm thick skin, the bottom part is the 20 mm thick chest wall; in between is the fatty breast tissue with a gland inside, and a 6 mm diameter tumour is assumed embedded in the breast. The dielectric properties of these tissues are listed in Table 1.

Table 1: Relative Permittivity and Conductivity of Breast Tissues [20].

	Relative Permittivity, ε_r	Conductivity, σ (S/m)
Fatty tissue	9	0.4
Skin	36	4
Glandular tissue	11–15	0.4–0.5
Chest wall	50	7
Tumour	50	4

The glands are modelled as circles with 10 mm radius or ellipses with 15 mm and 6.7 mm for the long and short axis, respectively.

2.3.2 3D Breast Phantom Models

The previous 2D phantom models are suitable for fast simulations used in feasibility studies. In order to test and compare the performance of recent UWB imaging techniques more realistic 3D models are required. Below is the description of two 3D models that have been recently published.

In [21] a simple hemisphere shape model with the most common dimensions is proposed (Figure 8). The breast diameter is 100 mm, the breast height is 60 mm, the skin thickness is 2 mm, and the chest thickness is 20 mm. The dielectric parameters of this model are summarized in Table 2, which are slightly different to those in Table 1. The tumour size ranges from 2 mm to about 15 mm or more, but 2.5 mm is the most commonly used value.

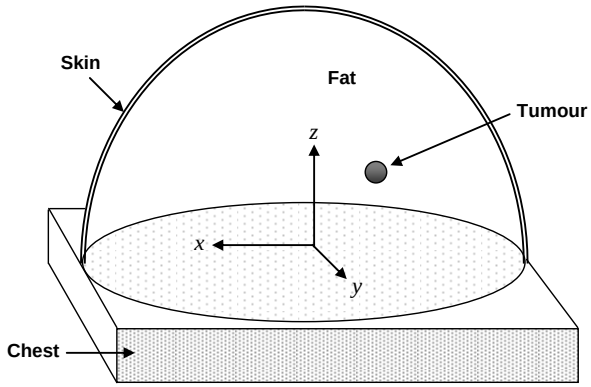

Figure 8: A Simple Hemispherical Brest Model.

Table 2: Relative Permittivity and Conductivity of Breast Tissues [21].

	Relative Permittivity, ε_r	Conductivity, σ (S/m)
Fat	5.14	0.14
Skin	37.9	1.49
Chest	53.5	1.85
Tumour	50	1.20

A more sophisticated model that includes randomly placed mammary glands is presented in [49] and extended in [50] (Figure 9). In this model, the glands are modelled as spheres with a radius between 8.5–12.5 mm and cylinders with radius between 2–18 mm and height between 12–27 mm. The tumour is modelled as a sphere with a diameter between 2–6 mm, embedded inside a gland, as this is the case for tumours in real life.

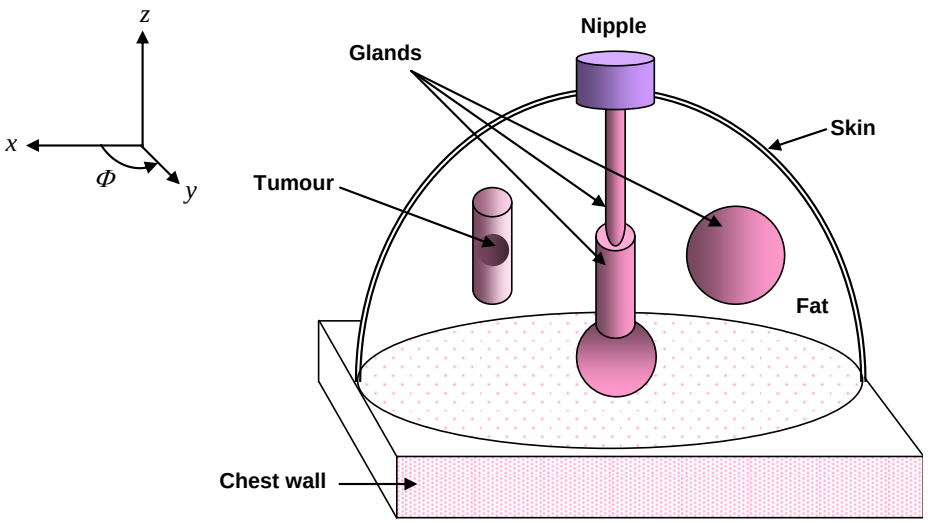

Figure 9: A Comprehensive Hemispherical Brest Model.

The base diameter of the breast is considered to be 140 mm and the skin is a 2 mm thick layer. The chest wall is a prism of 160×160×20 mm. The glands are randomly scattered throughout the fat tissue and

resemble real-case fibro-glandular tissue. Ducts can be added by assuming a cylindrical shape with a realistic configuration as shown in [50]. The electrical parameters for the different tissues considered in this model are summarized in Table 3.

Table 3: Relative Permittivity and Conductivity of Breast Tissues [50].

	Relative Permittivity, ε_r	Conductivity, σ (S/m)
Fatty tissue	9.8	0.4
Skin	34.7	3.89
Fibro-glandular tissue	21.5	1.7
Ducts	37.96	4.5
Chest wall	55.56	6.5
Nipple	45	5
Tumour	50	4

2.3.3 Research Perspectives

The feasibility of using UWB imaging techniques for the early detection of breast cancer has been proved in the multiple research works cited above. Recent results demonstrated the capability of detecting tumour sizes down to 2 mm in diameter [49], [50]; detection and accurate location of a 2.5 mm diameter tumour with 100% and 94.4% rate, respectively, were reported in [21]. These optimistic results encourage the improvement of the current UWB detection systems by optimizing the shape and amplitude of the transmitted pulses as well as the antenna design in order to increase the energy of the backscattered signals. Novel antenna topologies [50] might enable the development of ultra-sensitive diagnostic pouches around the breast thereby revolutionizing the breast cancer detection techniques. Nevertheless, future experiments need to be done on a standardized phantom model of the breast in order to assure fair comparison of different imaging techniques. To the best of our knowledge, the phantom model proposed in [50] (and its simplified version in [49]) is the most comprehensive one available in the literature and could be adopted as the reference model. The use of UWB images techniques can be combined with IR-UWB radar for the detection of morphological and physiological changes in the dermal tissues for skin cancer diagnosis too.

3.0 SENSOR LOCALIZATION AND TRACKING USING UWB SIGNALS

In many medical sensing applications, such as capsule endoscopy, the precise location of the sensor must be known for its data to be meaningful. The location of medical sensors in a WBAN must be estimated with millimetre-scale resolution. Localization in WSNs has been actively studied and several methods have been reported [51]–[55]. The dominant received-signal-strength-indicator (RSSI) technique consists in simply estimating the node distance by measuring the strength of the received signal. In a WSN, the distance to neighbouring nodes using RSSI is determined and then, by multiangulation or triangulation, relative localization of a specific node can be found and updated dynamically. Iterative algorithms exist to improve precision with increasing population of nodes [46]–[58]. Precision is, however, very poor with this method.

Several studies indicate that time-of-flight (TOF) measurements, combined with the good temporal resolution of IR-UWB, may improve precision. Measurements on the order of millimetres are reported in [51], but such method is not yet available in miniaturized, single-chip technology. In medical WBANs, minimal size is pivotal especially for devices operating inside the human body. Current localization technologies for WSNs have several shortcomings for medical applications. As computational resources

and power are limited in medical in-body sensors, difficult trade-offs between power emission, transmission bandwidth, and sensitivity must be resolved.

State-of-the-art 3D localization/tracking systems in the millimetre-scale have been reported in [59], [60]. In [59] a robust localization system is demonstrated using a DSSS transmission at 24 GHz with a bandwidth of 3.12 GHz. Although object tracking with an uncertainty of 0.1 mm is achieved by using a Kalman filter, the system's operation frequency is unsuitable for in-body transmissions due to the extremely high attenuation through living tissues at that part of the spectrum. A more convenient localization/tracking system for indoor WBANs that provides accuracy in the 1–10 mm range is described in [60]. This is achieved by transmitting a 300 ps Gaussian pulse, which is modulated by an 8 GHz carrier signal. In this system, the time-difference-of-arrival (TDOA) technique [58] is used and therefore four base stations are used for 3D localization. Due to its final dynamic accuracy of 5.86 mm and static accuracy of 3.86 mm obtained in a series of experiments, the system has been lauded as a milestone in UWB and wireless positioning systems.

3.1 Research Perspectives

UWB positioning technology demands extremely high speed signal processing with significant power efficiency. Furthermore, medical WBANs require miniature devices at low power consumption. Finding the best compromise between size, power, and localization accuracy is a major challenge. The so-called continuous-time binary value (CTBV) signal processing paradigm has demonstrated high speed sampling (>30 GHz). This might enable the implementation of novel accurate range measurement techniques such as the *active echo* paradigm [61], [62] for high precision localization of in-body sensors.

The active echo paradigm is based on TDOA using TOF measurements. This approach assumes that an EM token is actively returned with a known and possibly short delay (slave echo). When calculating TOF between two sensor nodes, the slave delay may be compensated for. This approach helps to tackle the problem of high attenuation of backscattered signals by human tissues that would exist in a passive echo radar approach. With EM waves travelling at the speed of light, high-speed sampling is required for good precision. An active echo engine (AEE) microchip can be integrated into on-body sensor radio transceivers, which can function as localization base stations, or can be used independently as a localization radar embedded in a recorded belt for a capsule endoscope system. If the AEE is combined with an IR-UWB communication transceiver, some basic circuits may even be shared.

However, in all the cases described so far, the complexity of body tissue introduces significant uncertainty to TOF estimations. Accurate knowledge of the propagation mechanism in different parts of the body is necessary in order to compensate for the difference of TOF measurements at different base stations caused by the different dielectric properties of the human tissues. This requires intensive simulation campaigns to determine the TOF variations in propagation through living tissues with respect to the free space.

4.0 WIRELESS BODY AREA NETWORK

The integration of on-body medical sensors, in-body sensors, and UWB radars into a single network requires a carefully planned architecture in order to guarantee proper operation without mutual interference between the different devices. The Federal Communication Commission (FCC) has allocated the 3.1–10.6 GHz frequency band for UWB communications in the United States [63]. It is important to notice, however, that a large part of this spectrum is strictly regulated in Europe and might not be available for new UWB radio systems. According to European regulations [64], [65] only the 6–8.5 GHz part of the spectrum is readily available for UWB transmissions with a maximum EIRP spectral density of –41.3 dBm/MHz without the use of interference mitigation techniques. Transmissions with the same spectral density are allowed in 3.4–4.2 GHz and 8.5–9 GHz for devices implementing the detect-and-avoid (DAA)

mitigation technique. Beyond December 31, 2010, the 4.2–4.8 GHz portion of the spectrum can be used if both DAA and low duty cycle (LDC) transmissions are implemented. This section provides a description of a viable communication configuration of a wireless body area network (WBAN) using UWB radio interfaces in the different allowed portions of the spectrum in Europe.

4.1 In-Body Sensor Interface

Our recent research on radio propagation inside the human body [28] reveals higher signal attenuation at higher frequencies. For instance, Figure 10 shows the average power density of several UWB signals below and above 1 GHz, respectively. The graphic was obtained by EM simulations of UWB signal propagating through the human chest. Both vertical polarization (VP) and horizontal polarization (HP) with respect to the standing body were considered. Notice that the 1–5 GHz signals are more severely attenuated than the 0.1–1 GHz ones. At higher frequencies the attenuation is even more severe.

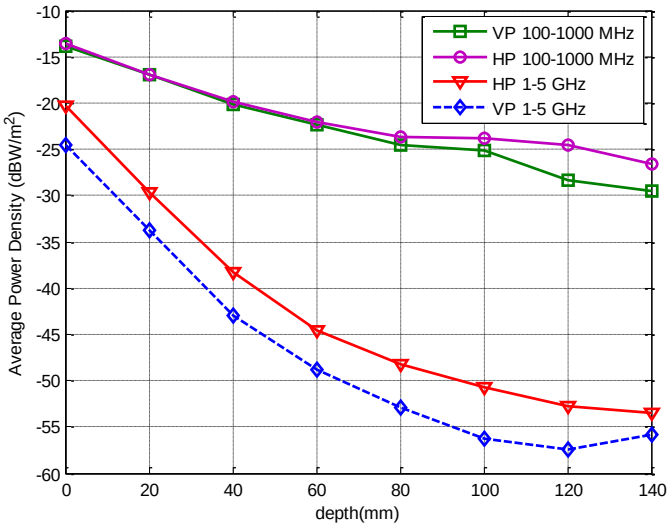

Figure 10: Average Power Density as a Function of Depth inside the Chest for Different Frequency Bands and Polarizations.

Since miniaturization and power consumption are the toughest design constraints for in-body sensors, the signal attenuation through living tissues must be the minimal possible. Therefore, the 3.4–4.8 GHz frequency band seems to be the most appropriate for these devices [66]. Although the regulations request the implementation of DAA and LDC in this portion of the spectrum, it is very unlikely that radio signals radiated from inside the human body at extremely low power can cause interference to other NB systems. In the case of full-duplex links, DAA and LDC can be implemented in the on-body transceiver where more complex circuitry can be afforded.

4.2 On-Body Sensor Interfaces

On-body medical sensors (motes) operate on or in very close proximity to the patient's skin (typically less than 2 centimeters). The communication requirements for on-body sensors are less stringent than in-body ones'. Typical data rate requirements for common medical sensing devices are given in [3]. It appears that electromyography (EMG) sensing is the most throughput-demanding (up to 1500 kbps) of the most common medical applications. However, it is important to note that continuous EMG monitoring is not necessary as is the case of electrocardiogram (ECG) and electroencephalogram (EEG). The former has a raw data rate requirement of 10–100 kbps whereas the former has 10–200 kbps. Conventional motes can benefit from UWB technology by having their NB communication radio interface replaced by an IR-UWB

transceiver. Currently, the IEEE 802.15.6 task group (http://www.ieee802.org/15/pub/TG6.html) is in the process of standardizing the characteristics of the UWB wireless interface for both on-body and in-body medical sensors. Independently of the standardization process, we have identified the 6–8.5 GHz spectrum portion as highly suitable for on-body sensors operation. Even more, the only portion of the UWB spectrum readily available worldwide is 7.25–8.5 GHz [65]; therefore, we strongly recommend adopting this frequency range for commercially standardized IR-UWB on-body transceivers. This will spare the implementation of DAA, thus keeping a low complexity of the motes' electronics. On-body channels are more prone to experience fading and larger RMS delay spread than in-body ones [67], thus an IR-UWB 7.25–8.5 GHz interface is expected to support low data rate only.

4.2.1 Relay Nodes

Because of the complex geometry of the human body, it is likely that some on-body nodes require the relaying of their data when a single-hop link cannot be established because of extremely high signal attenuation. A relay node (RN) fulfils this task using the same IR-UWB 7.25–8.5 GHz on-body interface. However, it is possible to include relaying capabilities in each mote's transceiver to ensure the establishment of multi-hop links whenever is required.

4.2.2 Gateway Nodes

In-body sensors will necessarily have their data relayed to a network controller for processing and displaying. This special relaying node has to be placed on the patient's skin (or very close to it). We refer to it as a gateway node (GN). A GN has special communication architecture because it must support two different (in-body and on-body) wireless interfaces. Depending on the kind of data transmitted by the in-body medical sensor, we can differentiate between low data rate gateway node (LDRGN) and high data rate gateway node (HDRGN). As mentioned in the subsection 2.1.3, we have demonstrated through simulations [29] that a high data rate in-body link can be established using IR-UWB. Therefore, the same IR-UWB 3.4–4.8 in-body GHz interface can be used to communicate an in-body sensor with its corresponding GN for either low or high data rate transmissions. However, the IR-UWB 7.25–8.5 GHz on-body interface supports only low data rate for data relaying (as mentioned above). Therefore, a LDRGN is any RN that supports both IR-UWB 3.4–4.8 GHz in-body and IR-UWB 7.25–8.5 GHz on-body interfaces for low data rates. In the case of a capsule endoscope with real-time video transmission, the on-body relaying interface must support high data rate transmissions. The ECM-368 interface [68], based on MB-OFDM, can support 480 Mbps at distances of up to 3 meters and 110 Mbps at up to 10 meters. The ECM-368 band can occupy the 6–7.25 GHz and 8.5–9 GHz, which roughly translates into subbands 7, 8, and 11, of the 14 ones in which the UWB spectrum is divided according to the ECM-368 standard. Therefore, a HDRGN supports both IR-UWB 3.4–4.8 GHz in-body and ECM-368 6–7.25/8.5–9 GHz on-body interfaces for high data rates. Since DAA is required in 8.5–9 GHz, this band should be occupied mainly for temporary transmissions such as capsule endoscopy and imaging.

4.3 Network Controller and Patient Monitor

The information collected by the low data rate sensors is gathered by a device referred to as *WBAN controller* (WBANC). The sensors are connected to the WBANC following a simple star network topology using the IR-UWB 7.25–8.5 GHz on-body interface (Figure 11). The WBANC, which can be devised as a personal digital assistant (PDA), executes a medium access control (MAC) algorithm to ensure that all the sensors transmit their information in an organized and fair way. For in-home healthcare, the WBANC can display several basic vital signals such as HR, BP, SpO2, etc. For in-hospital healthcare and surgery, a computer is used to process the information collected by the WBAN and other high data rate devices such as imaging radars and capsule endoscope systems. This computer is referred to as *patient monitor* (PM) and also displays the patient's physiological signals in a friendly manner. The WBANC and the imaging radars are connected to the PM using the ECM-368 radio interface.

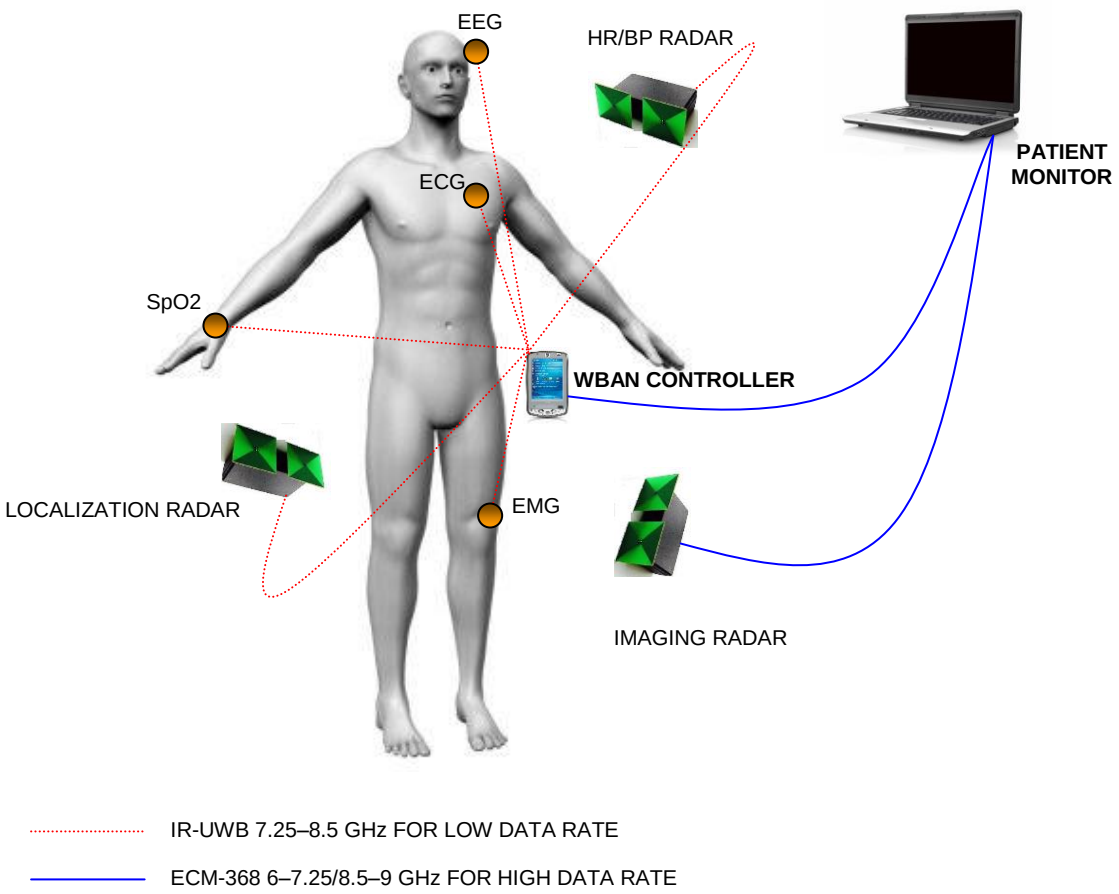

Figure 11: Network Topology of the On-Body WBAN.

As for in-body sensors, their GNs are connected either to the WBANC or directly to the PM depending on the information they transmit. LDRGNs are connected to the WBANC using the IR-UWB 7.25–8.5 GHz on-body interface whereas HDRGNs are connected to the PM through the ECM-368 interface (Figure 12). It is clear that the circuitry complexity of a HDRGN is high, which has a negative impact on its size; however, high data rate in-body sensors are expected to be used temporarily and generally during in-hospital healthcare (real-time capsule endoscopy session, for instance), hence the on-body device size is less critical in this case.

4.4 Research Perspectives

The network architecture presented above avoids mutual interference between the communication interfaces of the different medical WBAN components. Nevertheless, there are some interference issues that need to be addressed. The medical UWB radars used for sensing, imaging, and localization occupy generally a large portion of the spectrum too. While their communication interface has been specified, we still need to find the optimal frequency bandwidth for the pulses that are transmitted in the radar operation. This is not a trivial task, as several trade-offs must be considered (see subsection 2.2.2) together with the interference issues. Currently, the experiment medical radar used in our HR/BP research operates in 0.5–3 GHz; however, this frequency range covers very crowded frequency bands such as mobile telephony, so we plan on moving it within 3.1–10.6 GHz. For this sake, the inherent capability for frequency agility of the ECM-368 interface can be exploited. The core of any OFDM transceiver is an inverse/direct fast Fourier transform (IFFT/FFT) engine. It has been demonstrated that the FFT engine can be effectively

used as a spectrum analyzer with a frequency resolution of 4.125 MHz thereby facilitating the implementation of DAA algorithms [69], [70]. The EM coexistence with other radio systems such as WiMAX has to be evaluated through spectrum monitoring in the frequency ranges assigned to WBAN interfaces. The demonstration of a cognitive [71] medical WBAN is being pursued by our research group, and the Interventional Centre and the Norwegian Unuversity of Science and Technology (NTNU) are active in the COST Action IC0902 efforts towards the definition of a European platform for cognitive radio and networks (http://w3.cost.esf.org/index.php?id=110&action_number=IC0902).

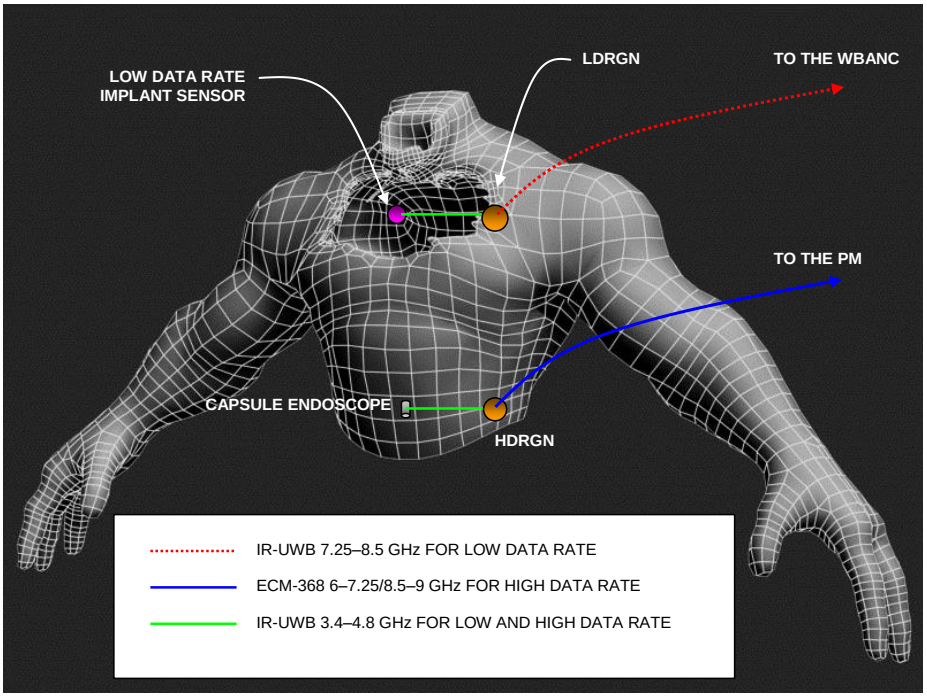

Figure 12: Network Topology of the In-Body WBAN.

5.0 CONCLUSIONS

Ultra wideband technology has many potential applications in medicine for less invasive medical diagnosis and monitoring. The UWB radar can potentially be used in novel noninvasive sensing and imaging techniques owing to its high temporal resolution for detecting backscattered signals. We have described our current research on the application of this technology to noninvasive measurement of blood pressure. The state of the art in UWB imaging for early breast cancer detection was also surveyed since it is a very promising application that can be extended to the detection of cancer in other parts of the body. Another application of UWB radar is the accurate localization of objects in the millimetre scale. This is particularly important for the real-time tracking of moving medical sensors that operate inside the human body such as capsule endoscopes.

The other aspect of UWB is its use as low-power-consuming wireless interface. Particularly, impulse radio seems to perfectly fit the communication requirements of tiny medical sensors, including in-body ones. Our research in this area was presented through the case study of a capsule endoscope system. Additionally, medical sensors and radars can be interconnected using UWB interfaces thereby enhancing the mobility of patients during surgery or intensive therapy. We described the integration architecture of all these systems into a single wireless body area network. One major issue to consider while interconnecting several medical devices using UWB radio interfaces is the possibility of mutual

interference with other systems that already operate in the 3.1–10.6 GHz frequency band. Therefore, new interference avoidance techniques and frequency agility such as cognitive radio have to be investigated.

The two aspects of UWB technology (radar and wireless interface) for medical applications are being investigated in Norway by the MELODY Project (http://www.melody-project.info/); MELODY stands for "medical sensing, localization, and communications using ultra wideband technology." The ultimate objective of this project is the improvement of current wireless health systems and the possible development of novel medical applications through UWB technology.

6.0 ACKNOWLEDGMENT

This work is part of the MELODY Project, which is funded by the Research Council of Norway under the contract number 187857/S10.

7.0 REFERENCES

[1] C. C. Chong, F. Watanabe, and H. Inamura, "Potential of UWB technology for the next generation wireless communications," in *Proc. 9th Intl. Symp. on Spread Spectrum Techniques and Applications (ISSSTA)*, Manaus, Amazon, Brazil, August 2006, pp. 422–429.

[2] J. Zhang, P. V. Orlik, Z. Sahinoglu, A. F. Molisch, and P. Kinney, "UWB systems for wireless sensor networks," *Proc. IEEE*, vol. 97, no. 2, pp. 313–331, February 2009.

[3] P. Gandolfo, D. Radović, M. Savić, and D. Simić, "IEEE 802.15.4a UWB-IR radio system for telemedicine," in *Proc. IEEE Intl. Conf. on Ultra-Wideband (ICUWB)*, Hannover, Germany, September 10–12, 2008, vol. 3, pp. 11–14.

[4] M. Hämäläinen, P. Pirinen, J. Iinatti, and A. Taparugssanagorn, "UWB supporting medical ICT applications," in *Proc. IEEE Intl. Conf. on Ultra-Wideband (ICUWB)*, Hannover, Germany, September 10–12, 2008, vol. 3, pp. 15–16.

[5] A. P. Chandrakasan, F. S. Lee, D. D. Wentzloff, V. Sze, B. P. Ginsburg, P. P. Mercier, D. C. Daly, and R. Blázquez, "Low-power impulse UWB architectures and circuits," *Proc. IEEE*, vol. 97, no. 2, pp. 332–352, February 2009.

[6] J. Ryckaert, C. Desset, A. Fort, M. Badaroglu, V. De Heyn, P. Wambacq, G. Van Der Plas, S. Donnay, B. Van Poucke, and B. Gyselinckx, "Ultra-wide-band transmitter for low-power wireless body area networks: design and evaluation," *IEEE Trans. Circuits Syst. I*, vol. 52, no. 12, pp. 2515–2525, December 2005.

[7] C. Y. Lee, and C. Toumazou, "Ultra-low power UWB for real time biomedical wireless sensing," in *Proc. IEEE Intl. Symp. Circuits Syst. (ISCAS)*, Kobe, Japan, May 23–26, 2005, pp. 57–60.

[8] M. M. Lee, E.-M. Lee, B. L. Cho, K. Eshraghian, and Y.-H. Kim, "The UTCOMS: A wireless video capsule nanoendoscope," *Progress in Biomedical Optics and Imaging*, vol. 7, no. 5, pp. 60820F.1–60820F.10, 2006.

[9] J. M. Herrerías, A. Caunedo, M. Rodríguez-Téllez, F. Pellicer, and J. M. Herrerías Jr., "Capsule endoscopy in patients with suspected Crohn's disease and negative endoscopy," *Endoscopy*, vol. 35, pp. 564–568, July 2003.

[10] M. Mylonaki, A Fritscher-Ravens, and P. Swain, "Wireless capsule endoscopy: A comparison with push enteroscopy in patients with gastroscopy and colonoscopy negative gastrointestinal bleeding," *GUT: Intl. J. of Gastroenterology and Hepatology*, vol. 52, pp. 1122–1126, August 2003.

[11] PHYsorg.com. (October, 2007). Capsule endoscopy turning up undiagnosed cases of Crohn's disease. [Online]. Available: http://www.physorg.com/pdf111757757.pdf

[12] X. Yong, L. Yinghua, Z. Hongxin, and W. Yeqiu, "An overview of ultra-wideband technique application for medial engineering," in *Proc. IEEE/ICME Intl. Conf. Complex Medical Engineering (CME)*, Beijing, China, May 23–27, 2007, pp. 408–411.

[13] E. M. Staderini, "UWB radars in medicine," *IEEE Aerosp. Electron. Syst. Mag.*, vol. 17, no. 1, pp. 13–18, January 2002.

[14] L-E. Solberg, I. Balasingham, S.-E. Hamran, and E. Fosse, "A feasibility study of aortic pressure estimation using UWB radar," in *Proc. IEEE Intl. Conf. on Ultra-Wideband (ICUWB),*Vancouver, Canada, September 9–11, 2009, pp. 464–468.

[15] W. Liu, H. M. Jafari, S. Hranilovic, and M. J. Deen, "Time domain analysis of UWB breast cancer detection," in *Proc. 23rd Biennial Symp. on Commun.*, Kingston, Canada, May 30–June 1, 2006, pp. 336–339.

[16] Y. Chen, E. Gunawan, Y. Kim, K. S. Low, C. B. Soh, and L. L. Thi, "UWB microwave breast cancer detection: Generalized models and performance prediction," in *Proc. IEEE Eng. Med. Biol. Soc. Conf. (EMBC)*, New York, NY, August 30–September 3, 2006, pp. 2630–2633.

[17] C. Yifan, E. Gunawan, K. Yongmin, L. Kaysoon, and S. Cheongboon, "UWB microwave imaging for breast cancer detection: Tumor/clutter identification using a time of arrival data fusion method," in *Proc. IEEE Antennas Propagat. Soc. Intl. Symp.*, Albuquerque, NM, July 9–11, 2006, pp. 255–258.

[18] C. C. Khor, and M. E. Bialkowski, "Investigations into an UWB microwave radar system for breast cancer detection," in *Proc. IEEE Antennas Propagat. Soc. Intl. Symp.*, Honolulu, HI, June 9–15, 2007, pp. 2160–2163.

[19] X. Xiao, and T. Kikkawa, "Early breast cancer detection by ultrawide band imaging with dispersion consideration," *Jpn. J. Appl. Phys.*, vol. 47, pp. 3209–3213, 2008.

[20] X. Xiao, and T. Kikkawa, "Influence of the organism interface on the breast cancer detection by UWB," *Applied Surface Science*, vol. 255, pp. 597–599, 2008.

[21] S. A. AlShehri, and S. Khatun, "UWB imaging for breast cancer detection using neural network," *Progress in Electromagnetic Research C*, vol. 7, pp. 79–93, 2009.

[22] S. H. Woo, K. W. Yoon, Y. K. Moon, J. H. Lee, H. J. Park, T. W. Kim, H. C. Choi, C. H. Won, and J. H. Cho. (2009, May). High speed receiver for capsule endoscope. *Journal of Medical Systems* [Online]. Available: http://www.springerlink.com/content/k221715t4810125g/fulltext.pdf

[23] T. Dissanayake, M. R. Yuce, and Chee Ho, "Design and evaluation of a compact antenna for implant-to-air UWB communication," *IEEE Antennas and Wireless Propagation Letters*, vol. 8, pp. 153–156, 2009.

[24] A. Khaleghi, and I. Balasingham, "Improving in-body ultra wideband communication using near-field coupling of the implanted antenna," *Microwave and Optical Technology Letters*, vol. 51, no. 3, pp. 585–589, March 2009.

[25] R. Gharpurey, and P. Kinget, U*ltra Wideband: Circuits, Transceivers and Systems*. New York, NY: Springer, 2008.

[26] H.-K. Chiou, and H.-J. Chen, "3.1–10.6 GHz ultra-wideband RF receiver in 0.18 μm CMOS technology," *Microwave and Optical Technology Letters*, vol. 52, no. 1, pp. 232–236, January 2010.

[27] P.-Z. Rao, T.-Y. Chang, C.-P. Liang, and S.-J. Chung, "An ultra-wideband high-linearity CMOS mixer with new wideband active baluns," *IEEE Trans. Microwave Theory Tech.*, vol. 57, no. 9, pp. 2184–2192, September 2009.

[28] A. Khaleghi, R. Chávez-Santiago, X. Liang, I. Balasingham, V. Leung, and T. A. Ramstad, "On ultra wideband channel modeling for in-body communications," in *Proc. IEEE Intl. Symp. on Wireless Pervasive Computing (ISWPC)*, Modena, Italy, May 5–7, 2010, to appear.

[29] A. Khaleghi, R. Chávez-Santiago, and I. Balasingham, "Ultra-wideband pulse-based data communications for medical implants," *IET Commun.*, to appear.

[30] M. O. Schurr, S. Schostek, C.-N. Ho, F. Rieber, and A. Menciassi, "Microtechnologies in medicine: An overview," *Minimally Invasive Therapy and Allied Technologies*, vol. 16, no. 2, pp. 76–86, 2007.

[31] G. Parati, G. Ongaro, G. Bilo, F. Glavina, P. Castiglioni, M. Di Rienzo, and G. Mancia, "Non-invasive beat-to-beat blood pressure monitoring: New developments," *Blood Pressure Monitoring*, vol. 8, no. 1, pp. 31–36, 2003.

[32] K. Matthys, and P. Verdonck, "Development and modelling of arterial applanation tonometry: A review," *Technology and Health Care*, vol. 10, no. 1, pp. 65–76, April 2002.

[33] J. Y. A. Foo, and C. S. Lima, "Pulse transit time as an indirect marker for variations in cardiovascular related reactivity," *Technology and Health Care*, vol. 14, no. 2, pp. 97–108, January 2006.

[34] G. Sharwood-Smith, J. Bruce, and G. Drummond, "Assessment of pulse transit time to indicate cardiovascular changes during obstetric spinal anaesthesia," *British Journal of Anaesthesia*, vol. 96, no. 1, pp. 100–105, October 2006.

[35] A. D. Droitcour, "Non-contact measurements of heart and respiration rates with a single-chip microwave doppler radar," Ph.D. dissertation, Dept. of Elect. Eng., Stanford Univ., June 2006.

[36] T. W. McEwan, "Body monitoring and imaging apparatus and method," US Patent 5573012, November 1996.

[37] I. Ya. Immoreev, "Ultra-wideband radars: features and ways of development," in *Proc. 2nd European Radar Conference (EuRAD)*, Paris, France, October 6–7, 2005, pp. 97–100.

[38] M. Sugawara, K. Niki, H. Furuhata, S. Ohnishi, and S. Suzuki, "Relationship between the pressure and diameter of the carotid artery in humans," *Heart and Vessels*, vol. 15, no. 1, pp. 49–51, September 2000.

[39] J. Lass, K. Meigas, D. Karai, R. Kattai, J. Kaik, and M. Rossmann, "Continuous blood pressure monitoring during exercise using pulse wave transit time measurement," in *Proc. of the 26th Annual Intl. Conf. of the IEEE Eng. Med. Biol. Soc. (IEMBS)*, San Francisco, CA, September 1–5, 2004, vol. 1, pp. 2239–2242.

[40] C. Gabriel, and S. Gabriel, "Compilation of the dielectric properties of body tissues at RF and microwave frequencies," Physics Dept., King's College, London, UK, Tech. Rep. WC2R 2LS, June 1996.

[41] C. G. Bilich, "Bio-medical sensing using ultra wideband communications and radar technology: A feasibility study," in *Proc. 1st Intl. Conf. on Pervasive Computing Technologies for Healthcare*, Innsbruck, Austria, November 29–December 1, 2006, pp. 1–9.

[42] A. Lazaro, D. Girbau, and R. Villarino, "Analysis of vital signs monitoring using an IR-UWB radar," *Progress in Electromagnetics Research*, vol. 100, pp. 265–284, 2010.

[43] J. M. Sill, and E. C. Fear, "Tissue sensing adaptive radar for breast cancer detection—Experimental investigation of simple tumor models," *IEEE Trans. Microwave Theory Tech.*, vol. 53, no. 11, pp. 3312–3319, November 2005.

[44] P. T. Huynh, A. M. Jarolimek, and S. Daye, "The false-negative mammogram," *Radiograph*, vol. 53, no. 5, pp. 1137–1154, September 1998.

[45] D. Li, M. Meaney, and K. D. Paulsen, "Conformal microwave imaging for breast cancer detection," *IEEE Trans. Microwave Theory Tech.*, vol. 51, no.4, pp. 1179–1186, April 2003.

[46] E. C. Fear, X. Li, S. C. Hagness, and M. A. Stuchly, "Confocal microwave imaging for breast tumor detection: Localization of tumors in three dimensions," *IEEE Trans. Biomed. Eng.*, vol. 49, no. 8, pp. 812–822, August 2002.

[47] E. J. Bond, X. Li, S. C. Hagness, and B. D. Van Veen, "Microwave imaging via space-time beamforming for early detection of breast cancer," *IEEE Trans. Antennas Propagat.*, vol. 51, no. 8, pp. 1690–1705, August 2003.

[48] S. K. Davis, H. Tandradinata, S. C. Hagness, and B. D. Van Veen, "Ultrawideband microwave breast cancer detection: A detection-theoretic approach using the generalized likelihood ratio test," *IEEE Trans. Biomed. Eng.*, vol. 52, no. 7, pp. 1237–1250, July 2005.

[49] N. Tavassolian, S. Nikolaou, and M. M. Tentzeris, "Microwave tumor detection using a flexible UWB elliptical slot antenna with a tuning uneven U-shape stub on LPC," in *Proc. IEEE Antennas Propagat. Soc. Intl. Symp.*, Honolulu, HI, June 9–15, 2007, pp. 257–260.

[50] N. Tavassolian, S. Nikolaou, and M. M. Tentzeris, "A flexible UWB elliptical slot antenna with a tuning uneven U-shape stub on LPC for microwave tumor detection," in *Proc. of Asia-Pacific Microwave Conf. (APMC)*, Bangkok, Thailand, December 11–14, 2007.

[51] M. Tuchler, V. Schwarz, and A. Huber, "Location accuracy of an UWB localization system in a multi-path environment," in *Proc. IEEE Intl. Conf. on Ultra-Wideband (ICUWB)*, Zurich, Switzerland, September 5–8, 2005, pp. 414–419.

[52] M. Baunach, R. Kolla, and C. Mvihlberger, "Beyond theory: Development of a real world localization application as low power WSN," in *Proc. IEEE Conf. on Local Computer Networks*, Dublin, Ireland, October 15–18, 2007, pp. 872–884.

[53] F. Sottile, and M. A. Spirito, "Robust localization for wireless sensor networks," in *Proc. 5th Annual IEEE Commun. Society Conf. on Sensor, Mesh and Ad Hoc Commun. And Networks (SECON),* San Francisco, CA, June 16–20, 2008, pp. 46–54.

[54] M. R. Mahfouz, Z. Cemin, B. C. Merkl, M. J. Kuhn, and A. E. Fathy, "Investigation of high-accuracy indoor 3-D positioning using UWB technology," *IEEE Trans. Microwave Theory Tech.*, vol. 56, no. 6, pp. 1316–1330, June 2008.

[55] H. A. Hjortland, and T. S. Lande, "CTBV integrated impulse radio design for biomedical applications," *IEEE Trans. Biomed. Circuits Syst.*, vol. 3, no. 2, pp. 79–88, April 2009.

[56] N. Patwari, J. N. Ash, S. Kyperountas, A. O. Hero III, R. L. Moses, and N. S. Correal, "Locating the nodes: Cooperative localization in wireless sensor networks," *IEEE Signal Processing Mag.*, vol. 22, no. 4, pp. 54–69, July 2005.

[57] H. Wymeersch, J. Lien, and M. Z. Win, "Cooperative localization in wireless networks," *Proc. IEEE*, vol. 97, no. 2, pp. 386–403, February 2009.

[58] S. Gezici, and H. V. Poor, "Position estimation via ultra-wide-band signals," *Proc. IEEE*, vol. 97, no. 2, pp. 427–450, February 2009.

[59] C. Meier, A. Terzis, and S. Lindenmeier, "A robust 3D high precision radio location system," in *Proc. IEEE/MTT-S Intl. Microwave Symp.,* Honolulu, HI, June 3–8, 2007, pp. 397–400.

[60] M. Kuhn, C. Zhang, M. Mahfouz, and A. E. Fathy, "Real-time UWB indoor positioning system with millimeter 3-D dynamic accuracy," in *Proc. IEEE Antennas Propagat. Soc. Intl. Symp.*, Charleston, CS, June 1–5, 2009.

[61] H. K. Olafsen, "Wireless sensor network localization strategies," M.Sc. thesis, Dept. Informatics, Univ. of Oslo, Norway, 2007.

[62] N. Andersen, "Active echo high precision ranging in wireless sensor networks," M.Sc. thesis, Dept. Informatics, Univ. of Oslo, Norway, 2007.

[63] *First report and order, revision of part 15 of the commission's rules regarding ultra-wideband transmission systems*, FCC, ET Docket 98-153, 2002.

[64] E. Faussurier. (2008, September 12). Spectrum management and ultra-wideband (UWB) [Online]. Available: http://www.icuwb2008.org/files/files/pdf/Article-IEUWB_EFA-12sept2008.pdf

[65] H.-B. Li, "Body area network—Standardization and technology," presented at the 2nd Intl. Symp. on Applied Sciences in Biomedical and Commun. Technol. (ISABEL), Bratislava, Slovak Republic, November 24–27, 2009.

[66] Q. Wang, K. Masami, and J. Wang, "Channel modeling and BER performance for wearable and implant UWB body area links on chest," in *Proc. IEEE Intl. Conf. on Ultra-Wideband (ICUWB),*Vancouver, Canada, September 9–11, 2009, pp. 316–320.

[67] *Channel Model for Body Area Network (BAN)*, IEEE P802.15-08-0780-09-0006, April 27, 2009.

[68] *High Rate Ultra Wideband PHY and MAC Standard*, ECMA-368 Standard, December 2008.

[69] A. Batra, S. Lingam, and J. Balakrishman, "Multi-band OFDM: A cognitive radio for UWB," in *Proc. IEEE Intl. Symp. Circuits Syst. (ISCAS)*, Island of Kos, Greece, May 21–24, 2006, pp. 4094–4097.

[70] J. Lansford, "The WiMedia UWB radio: Is it the ideal cognitive radio processor?," in *Proc. IEEE Intl. Conf. on Ultra-Wideband (ICUWB)*, Hannover, Germany, September 10–12, 2008, vol. 2, pp. 173–176.

[71] N. Devroye, M. Vu, and V. Tarokh, "Cognitive radio networks," *IEEE Signal Processing Mag.*, vol. 25, no. 6, pp. 12–23, November 2008.